PHYSICAL REVIEW B VOLUME 18, NUMBER 8 15 OCTOBER 1978

Cation interstitial pair modes in the vibrational spectra of mixed β-aluminas

P. B. Klein, D. E. Schafer,* and U. Strom
Naval Research Laboratory, Washington, D. C. 20375
(Received 24 May 1978)

Raman and far-infrared measurements of the cation vibrational spectra of the mixed systems $Na_{1-x}K_x$ and $Na_{1-x}Rb_x$ β-alumina were carried out at 300 K. The composition dependences of the observed spectral features were used to assign those features to specific types of cation sites. The resulting assignments indicate that many of the main features of the vibrational spectra below 120 cm^{-1} may be attributed to vibrations of interstitial cation pairs of the kind suggested by Whittingham and Huggins to account for fast ion diffusion in the β-aluminas (interstitialcy mechanism). Other regions of the vibrational spectra are attributed to unpaired cations. These results provide experimental evidence for the existence of these pairs and thus verify a central feature of the interstitialcy mechanism.

I. INTRODUCTION

Numerous theoretical and experimental investigations have been directed toward understanding the unusually high ionic mobilities of various cations in β-alumina. Of the many ideas that have emerged in descriptions of the ionic transport, the most successful has been the interstitialcy mechanism proposed by Whittingham and Huggins[1] and treated quantitatively by Wang, Gaffari, and Choi[2] (WGC). This mechanism for ionic diffusion involves the hopping of ions between the so-called mid-oxygen (mid-O) interstitial sites, which are known from structural determinations[3] to be partially occupied. These sites appear to take up the inherent nonstoichiometric excess (25%–30%) of cations found in all known β-aluminas. The calculations of WGC predict that stable occupation of the mid-O interstitial sites can only occur for pairs of interstitial mid-O cations straddling an empty regular cation site [Beevers-Ross (BR) site]. The low thermal activation energies for ionic diffusion observed experimentally (~0.16 eV for Na β-alumina) are then accounted for quantitatively by a correlated hopping process, in which one cation of an interstitial pair hops toward an adjacent singly occupied BR site, forming a new interstitial pair there and leaving behind a singly occupied BR site. Negligible contribution to the ionic diffusion was attributed to hops of unpaired cations between BR sites, since very high thermal activation energies (~2 eV) were calculated for that process.

Measurements of vibrational spectra such as those described here do not directly probe the ionic diffusion, but still have a bearing on our understanding of the ionic transport by characterizing the state of the mobile ion in the time between hops. Features of the Raman[4,5] and infrared[6-9] spectra that are sensitive to cation substitution in the isomorphic series Na, K, and Rb β-alumina and in Ag β-alumina have been identified as involving predominantly cation vibrational motion. The fact that these cation modes lie at frequencies lower and well separated from other substitution-insensitive modes has been shown to indicate that the cations are relatively weakly bound to the β-alumina host structure.[7] In the present work, some of the features of the vibrational spectra of mixed alkali ion-substituted β-aluminas are shown to be consistent with the motion of correlated interstitial cation pairs, similar to that discussed by WGC. These measurements thus provide experimental evidence for the existence of these correlated ion pairs in the β-aluminas.

The crystal structure of β-alumina was determined by Bragg *et al.*[10] and Beevers *et al.*,[11,12] and was refined by Peters *et al.*[3] The material forms a layered structure characterized by loosely packed planes containing all of the cations, thus accounting for the characteristic two-dimensional ionic conductivity. These planes are separated by close-packed spinel-like blocks of aluminum and oxygen, four oxygens thick (referred to as "spinel blocks"). The center of each conducting plane forms a mirror plane for the spinel blocks above and below it. The spinel blocks are bound together by oxygens in the conducting plane via Al–O–Al bonds and also by the cations in the plane. In the ideal (stoichiometric) material, $Na_2O \cdot 11Al_2O_3$, the cations (all on BR sites and all BR sites filled) and the in-plane oxygens form a loosely packed hexagonal lattice with a lattice constant of 5.58 Å, as shown in Fig. 1. The actual structure, however, contains numerous defects due to the excess cations. In the cases of all the alkali-metal β-aluminas, the excess cations reside predominantly on the interstitial mid-O sites, and according to the calculation of WGC, occupy such sites in pairs straddling empty BR sites, as shown in Fig. 1. Thus approximately 25% of the BR sites of the ideal structure become doubly occupied with interstitial pairs. A second

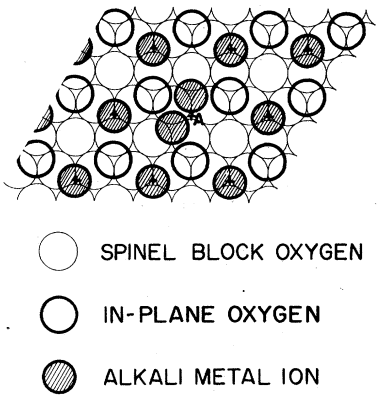

FIG. 1. Structure of β-alumina in the diffusing plane. The light circles are spinel-block oxygens above and below the plane, while the heavy circles are oxygens within the plane. The shaded circles are the metal ions. BR sites are marked with a (+), and a mid-O pair is shown near the point A.

type of interstitial site, the anti-BR site, is essentially unoccupied in all β-aluminas (except Ag β-alumina) due to the close proximity of this site to nearby spinel-block oxygens.

In addition to the excess metal ions, further defects must be present in the structure in order to satisfy charge neutrality. There is evidence[13] that these compensating defects take the form of excess O^{2-} occupying in-plane mid-O sites and bound by two Al^{3+} Frenkel defects. Thus the conducting plane is characterized by a significant amount of structural disorder introduced by both excess metal ions and charge-compensating defects. Microwave measurements,[8,14] diffuse x-ray scattering,[15-18] NMR,[19] and thermal measurements[20,21] have been used to investigate the role of disorder in the ion diffusion process as well as the extent of local ordering of the defect arrangement. The results of these measurements indicate (i) a distribution of barrier heights for ion hopping and (ii) some local ordering of the cations with ion-ion correlation lengths increasing with ionic radius.

The ion-ion correlations deduced from the diffuse x-ray-scattering measurements have been interpreted in terms of a structural model for the nonstoichiometric material incorporating extended order and an enlarged unit cell.[15-18] The proposed unit cell of the resulting superlattice, three times larger than that of the stoichiometric material, contains in each layer two metal ions in BR sites and two metal ions forming an interstitial pair about a third (vacant) BR site. Due to the lack of long-range order, however, the superlattice structure would only be expected to exist in the form of locally ordered regions, or microdomains.

The distribution of barrier heights, a reflection of the disorder in the conducting plane, is expected to contribute to some extent to the linewidth of the cation vibrational spectra,[8] but not significantly to the frequencies or relative intensities of the vibrational modes. Ion-ion correlations, however, are indicative of the degree of local ordering, and may be an important factor in determining the form of the vibrational spectra associated with the metal ions.

The occupation of a large number of interstitial sites by metal ions would generally be expected to have a significant effect upon the vibrational spectra. On the other hand, by considering the symmetry properties of the superlattice, Hao *et al.*[5] have interpreted the spectral features observed in the Raman measurements of some of the β-alumina isomorphs as being due entirely to vibrations of ions in BR sites within a superlattice structure. No contributions to the vibrational spectra could be attributed to the motion of correlated ion pairs. However, a calculation[22] of the vibrational spectra of the metal ions (also assuming a superlattice) indicates that some of the observed spectral features can be interpreted as due to the in-phase motion of correlated ion pairs. The calculated spectra compare well with experiment. The latter view has also been supported by a comparison of Raman and far-infrared measurements.[9]

In the present work, the existence of correlated ion-pair vibrations is investigated through a study of the composition dependence of the Raman and far-infrared spectra of the mixed cation systems $Na_{1-x}K_x$ and $Na_{1-x}Rb_x$ β-alumina. In these two-component systems, the model employed by WGC leads to three types of cation interstitial pairs that can occur (neglecting charge-compensating defects): Two types of "pure" pairs and one type of "mixed" pair. The approach taken in the present analysis of the vibrational spectra is to assume that each of the observed infrared- and Raman-active cation vibrational modes arises either from one of these three types of pairs or from one of the two possible types of singly occupied BR sites, and to assign the observed spectral features according to the distinctly different composition dependences expected for each type of site. This procedure also assumes that the observed intensity of the vibrational mode of a given type of site depends predominantly on the number of such sites present. The validity of this assumption is supported by the observation that the composition dependence of corresponding Raman scattering and infrared absorption spectra appears to be remarkably similar in spite of the differences between the two physical processes.

In Sec. II, the experimental details are described, followed in Sec. III by a presentation of the experimental results of the Raman and infrared measurements. The analysis and discussion of the data appear in Sec. IV, and a brief conclusion follows in Sec. V.

II. EXPERIMENTAL

All samples used in the far-infrared and Raman measurements were cut from one large single crystal of melt-grown Na β-alumina obtained from the Union Carbide Corp. Two samples were used for the far-ir transmission measurements. These were cut with a wire saw to approximately 10×10 mm and polished down to thicknesses (along the c axis) of 58 and 105 μm, using 1-μm Al_2O_3 abrasive for the final polishing step. Samples for the Raman measurements were cut into rectangular parallelipipeds $10\times 10\times 1$ mm . Cut surfaces normal to the x-y plane were polished to an optical finish for the incident laser beam, while natural (cleaved) surfaces parallel to the x-y plane were employed to view the light scattered from the sample. The mixed β-aluminas were prepared from the original Na β-alumina composition by ion exchange. Following Yao and Kummer[23] and Kummer,[24] the ion exchanges were carried out by immersing the Na β-alumina samples in the proper molten $NaNO_3$-KNO_3 or $NaNO_3$-$RbNO_3$ mixtures at 350 °C for approximately 72 h. The set of two far-ir transmission samples was sequentially ion exchanged and measured at K mole fractions of 0, 0.11, 0.30, 0.50, 0.70, 0.86, and 1.0 in the order listed.

The far-ir transmission and reflectivity measurements were carried out at room temperature using an RIIC model FS-720 Fourier transform spectrometer. The far-ir light was detected with a Ge:Ga bolometer (Infrared Industries, Inc.) held at 4.2 K. Multiple scanning, data processing, and Fourier transformation were carried out with a Nicolet 1070 multichannel analyzer (MCA) controlled by a PDP-8/e minicomputer. Each β-alumina sample spectrum was normalized to the spectrum of an empty aperture taken immediately before or after the sample spectrum. The resulting far-ir conductivity values were mainly sensitive to the transmission measurements, since the samples were fairly opaque ($T<0.2$). The reflectivity measurements were used to correct for reflection losses and the effects of multiple internal reflections at the higher transmission values. In addition, the reflectivity spectra were compared to the Kramers-Kronig transform of the conductivity spectra. Consistency between the two spectra was observed in all cases. Based upon the results of repeated transmission measurements on a given sample, the uncertainty in the measured transmission was found to correspond to maximum errors in the conductivity of approximately $\pm$ 1$(\Omega\,\mathrm{cm})^{-1}$ in regions of high conductivity (peaks) and ± 0.2 $(\Omega\,\mathrm{cm})^{-1}$ in regions of low conductivity.

The Raman measurements were made at room temperature in a standard 90° scattering geometry, with the incident laser radiation propagating normal to the $\hat{c}$ axis and the electric vector linearly polarized in the x-y plane. The scattered light was observed along the $\hat{c}$ axis, with the polarization totally in the x-y plane. Steps were taken to ensure that the scattering geometry was identical for all of the samples (compositions) measured. This is an important point, since, as discussed below, the Raman intensities of the cation modes were measured relative to the intensity of a spinel-block mode which is sensitive to the scattering geometry through polarization selection rules.

Rather than attempt absolute-intensity measurements of the cation vibrational modes for the various samples, we chose the 259-cm^{-1} mode of the Na-K mixed system (associated mostly with internal spinel-block vibrations) as a reference because of its strength and narrow spectral width (thus allowing rapid data acquisition) and its relative insensitivity to cation substitution. This mode was measured simultaneously with the cation modes for each sample, so that Raman intensities of the cation modes were determined relative to the 259-cm^{-1} mode intensity. A single careful set of absolute-intensity measurements of the 259-cm^{-1} mode indicated that the integrated intensity is essentially independent of sample composition.

The Raman measurements were obtained using several laser lines from a 4-W Ar^+ ion laser (Coherent Radiation). The scattered light was dispersed with a Jarrell-Ash 100-25 double spectrometer and was detected with a cooled RCA 31034A photomultiplier. The photomultiplier output was processed by standard photon counting electronics and stored in a Nicolet 1070 MCA. The instrumental width of the spectrometer was approximately 2 cm^{-1}.

The pure β-aluminas (Na, K, and Rb) were each measured separately with 4579-Å excitation, since several Ar emission lines fall in convenient positions for use as absolute-frequency calibrations. The frequencies of the Raman peaks (± 1 cm^{-1}) could thus be accurately compared to those of previously published measurements.

III. VIBRATIONAL SPECTRA

The Raman and far-ir measurements were carried out at room temperature. The Raman spectra for the Na-K mixed system in the region of the cation vibrational modes are shown in Fig. 2 for several representative values of potassium con-

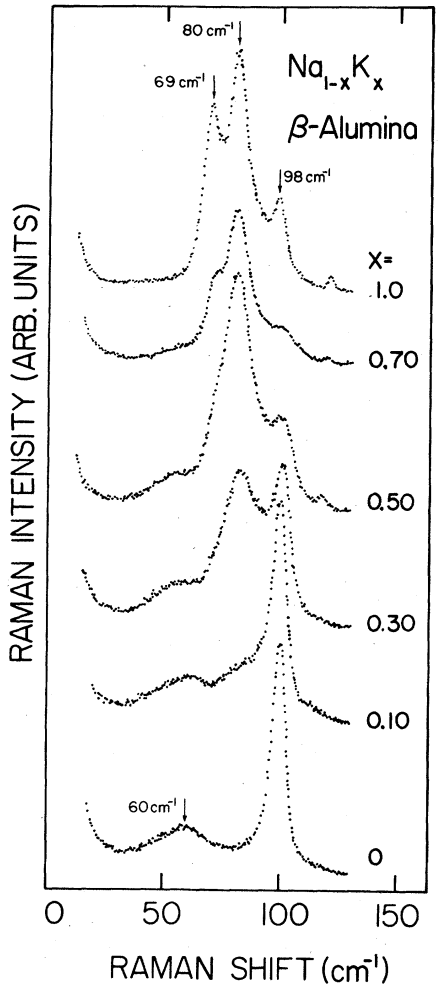

FIG. 2. Raman spectra of the cation vibrational modes for the $Na_{1-x}K_x$ β-alumina mixed system. The intensity scales for each of the spectra are generally different (within about a factor of 2). Normalization of the Raman intensities is discussed in the text. Instrumental width is approximately 2 cm^{-1}.

centration x. Dramatic changes in the relative intensities of the different modes are observed as the sample composition is varied. In the figure, absolute intensities should not be compared directly between different spectra, since the intensity scales for each of the spectra are somewhat different (within about a factor of 2). The K β-alumina spectrum is dominated by three modes at 69, 80, and 98 cm^{-1}, while the Na β-alumina spectrum exhibits one broad mode centered at 60 cm^{-1} and a sharper mode at 99 cm^{-1}. (For convenience, vibrational modes will be labeled and referred to according to their frequencies in the *pure* β-alumina, even though their frequencies are observed to vary somewhat with composition.) These results are in agreement with previous Raman work,[4,5] although the frequencies measured for some of the modes differ slightly (1–4 cm^{-1}). Since it appears in all of the β-alumina isomorphs, the Raman peak near 100 cm^{-1} is not considered to be strictly due to a cation vibrational mode,[5] although the effect of the ion species on the Raman intensity is significant. The replacement of K^+ by Na^+ is seen to have a dramatic effect on the relative intensity of the two K^+ modes at 69 and 80 cm^{-1} — the strength of the lower-frequency mode decreases rapidly with decreasing K^+ content, and has almost vanished by the time 50% of the K^+ ions have been replaced. This distinct difference in composition dependence for two modes of the same cation species (K^+) is the first indication that vibrations of more than one type of site are contributing to the Raman spectra.

The corresponding far-ir spectra for the mixed Na-K β-alumina system are shown in Fig. 3 for several values of sample composition. The K^+

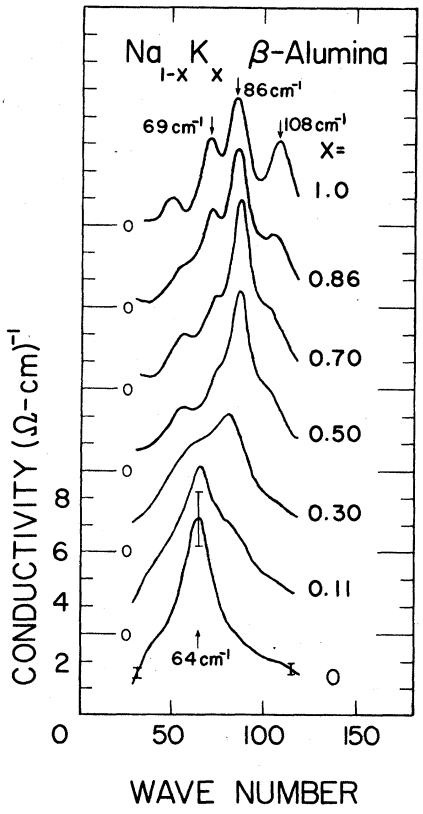

FIG. 3. Far-infrared spectra of the cation vibrational modes for the $Na_{1-x}K_x$ β-alumina mixed system. The zero of the conductivity for each spectrum is shifted by 3 $(\Omega\,cm)^{-1}$. The error bars indicate the maximum uncertainties in conductivity in the low- and high-transmission regions.

spectrum is characterized by three modes of 69, 86, and 108 cm^{-1}, and the Na^+ spectrum is dominated by a broad mode at 64 cm^{-1} and a very broad high-frequency tail in the 80–120-cm^{-1} region. An additional mode is observed at 50 cm^{-1} at high K concentration, but the origin of this mode is not yet understood. Comparison with Fig. 2 indicates that the far-ir spectra are remarkably similar to the Raman spectra, although part of this similarity is fortuitous, since the 108-cm^{-1} infrared mode will be shown to have no correspondence to the 98-cm^{-1} Raman mode. Nonetheless, the relative strengths of the 69- and 86-cm^{-1} infrared modes exhibit the same dramatic dependence upon sample composition as their 69- and 80-cm^{-1} Raman counterparts. This similarity between the Raman and far-ir spectra indicates that it is unlikely that the observed dependence upon K concentration is related to a composition dependence of the appropriate transition matrix elements. These would not generally be expected to exhibit similar behavior for both infrared absorption and Raman processes. The observed composition dependences are thus attributed to the associated variations in the numbers of ions occupying different sites.

In order to verify some of the trends observed in the Na-K mixed system with varying composition, a limited Raman study of the Na-Rb system was undertaken and compared to the far-ir measurements of Allen *et al.*[9] in Rb β-alumina. These results are shown in Fig. 4. The far-ir spectrum is shown as the solid line in Fig. 4(a). The Raman spectra for Rb, $Na_{0.5}Rb_{0.5}$, and Na β-alumina are shown in Figs. 4(b), 4(c), and 4(d), respectively. The Rb Raman spectrum is in essential agreement with previously published data,[5] although the frequencies determined in the present measurements are 4–7 cm^{-1} lower than those previously reported. This discrepancy is well outside experimental error. The correspondence between the far-ir and Raman spectra as observed in the Na-K system (Figs. 2 and 3) is seen to extend to the Na-Rb system as well; the Rb Raman modes at 59 and 65 cm^{-1} appear at 61 and 73 cm^{-1} in the far-ir spectrum. A careful Raman measurement of the Rb spectrum above 75 cm^{-1} [Fig. 4(b)] verifies the existence of a weak mode near 90 cm^{-1}. The position of this Raman mode corresponds well with the strong infrared mode at 87 cm^{-1}. In addition, it is also apparent from Fig. 4 that, unlike the Na-K system, the 98-cm^{-1} Raman mode frequency is sensitive to sample composition in the Na-Rb system; its frequencies for 0%, 50%, and 100% Rb appear at 99, 105, and 112 cm^{-1}, respectively.

The most striking feature of the Raman spectra in the Na-Rb system, however, is that the intensities of the 59- and 65-cm^{-1} Rb Raman modes

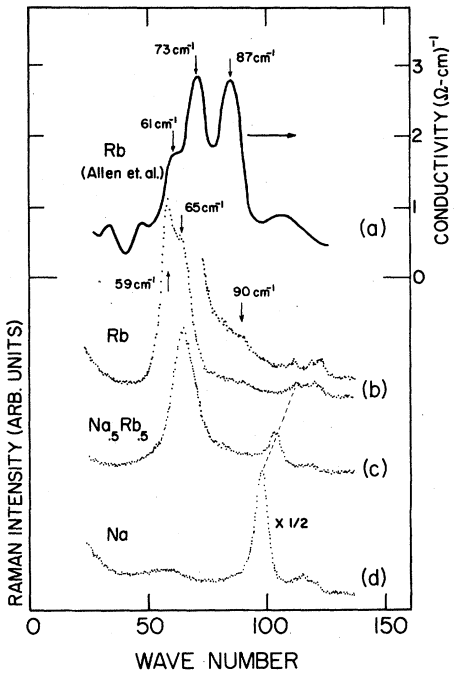

FIG. 4. (a) Rb β-alumina far-ir spectrum of Allen *et al.* (Ref. 9); (b)–(d) Raman spectra of Rb, $Na_{0.5}Rb_{0.5}$, and Na β-alumina. The upper Rb spectrum in (b) was taken at higher sensitivity. The dashed line indicates the composition dependence of the 99-cm^{-1} mode of the Na spectrum.

exhibit the same dramatic dependence upon concentration as the corresponding K Raman modes (69 and 80 cm^{-1}) in Fig. 2; with decreasing Rb concentration the lower-frequency mode drops rapidly in intensity relative to the higher-frequency mode. It is clear from this correspondence that the same types of sites are contributing to this portion of the spectrum in both K and Rb β-alumina.

IV. ANALYSIS AND DISCUSSION

The features of the vibrational spectra of the Na-K and Na-Rb mixed β-aluminas will now be analyzed in terms of the various possible occupations of cation sites implied by the interstitialcy model (e.g., Na-Na, Na-K, and K-K pair sites or singly occupied Na or K sites). Such an approach assumes that the cation vibrations are separable into modes involving the motion of ions on a single type of site, and that the variation of a mode intensity (Raman or infrared) with composition depends predominantly on the variation in the number of that type of site. The assumption of separability is supported qualitatively by calculations of the β-alumina phonon spectrum, and the as-

sumption relating intensities directly to numbers of occupied sites is supported by the similar composition dependency of the intensities of the Raman and far-ir spectra, as discussed previously. The approximate separability of modes arises because the nearest neighbors of the cation(s) at a given site consist of relatively tightly bound spinel-block and in-plane oxygen ions which tend to define a spring constant for motion of the cations relative to the spinel block. Adding cation-cation coupling due to the direct Coulomb interaction leads to relatively distinct pair and single-ion modes, with[25] or without[22] the polarization response of the nearby spinel-block ions taken into account.

In order to assign the observed cation vibrational modes to particular types of sites on the basis of their compositional dependence, a model for the relative number of each type of site as a function of composition is required. In the absence of any energetic preference of one of these types of sites over another, the distribution of cations among the different types of sites would be random, resulting in x (mole fraction K or Rb) dependence as listed in Table I for the case of N BR sites and a cation excess of 25%. For different amounts of cation excess the prefactors in Table I would vary, but the functional dependence upon x would remain the same. If any type of site is energetically favored over the others, however, the x dependence will deviate from those given, to an extent which is dependent upon the relative magnitudes of the energy preference and kT.

A. Doubly occupied sites

The Raman and infrared spectra presented in the preceding section for the mixed Na-K system have been analyzed in detail by decomposing the spectra into a sum of Lorentzians, using a modified least-squares-fitting program.[26] The resulting fitting parameters provided the dependence upon sample composition of the linewidth, frequency, and intensity of each of the component lines. The resulting frequencies of the component Lorentzians are plotted versus composition in Fig. 5. This figure illustrates quantitatively the correspondence between Raman- and infrared-active modes described in Sec. III. The 60-cm^{-1} (Na), 69-cm^{-1}, and 80-cm^{-1}(K) Raman frequencies consistently lie 2–5 cm^{-1} below their infrared counterparts at compositions where the latter are clearly distinguishable. Corresponding far-ir and Raman modes thus have very similar composition dependence. Such Raman-infrared splittings are comparable to those estimated by Barker *et al.*[7] for cation vibrational modes based on the indirect coupling (via the spinel block) of neighboring diffusing planes. The lack of correspondence (Fig. 5) between the Raman and infrared K modes at 98 and 108 cm^{-1}, respectively, stems from the fact that the 98-cm^{-1} Raman mode is not strictly a cation vibration, but is rather a coupled mode involving the cation and in-plane oxygens.[5,7] The

TABLE I. Composition dependence of the occupancy of the various sites in $Na_{1-x}K_x$ β-alumina assuming 25% excess cations and random occupation of excess ions on lattice sites. N is the total number of regular cation lattice sites and x is the mole fraction K^+ (or Rb^+ in the Na-Rb mixed system).

Type of site	Number of sites	Cations/site
Singly occupied sites:		
K^+	$\frac{3}{4}Nx$	1
Na^+	$\frac{3}{4}N(1-x)$	1
Doubly occupied sites:		
K^+-K^+	$\frac{1}{4}Nx^2$	2
Na^+-Na^+	$\frac{1}{4}N(1-x)^2$	2
Na^+-K^+	$\frac{1}{4}N[2x(1-x)]$	2

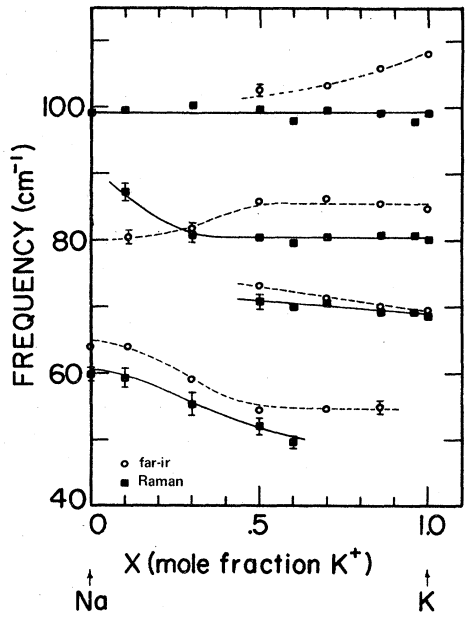

FIG. 5. Composition dependence of the frequencies of the Raman (squares) and infrared (circles) modes in the Na-K mixed system, as determined by the computer decomposition of the vibrational spectra. Error bars indicate the uncertainty in the fitting parameters, and are shown explicitly when their values are significantly larger than the size of the data points. The solid (Raman) and dashed (infrared) lines have been included for clarity, and are not fits to any particular model.

Raman intensities of the cation modes were measured relative to the 259-cm^{-1} phonon, as discussed in Sec. II. The dependence of the absolute Raman intensity of this phonon upon sample composition was measured separately, and the result is shown in the upper portion of Fig. 6. The integrated Raman intensity of the 259-cm^{-1} mode is essentially independent of sample composition. The 15%–20% scatter in the data points is characteristic of absolute-intensity measurements, especially since each point corresponds to a measurement in a different sample. The relative-intensity measurements, however, are expected to be significantly better than this, and in many cases the error bars are dominated by the uncertainties in the fitting parameters obtained by the computer decomposition.

The two sets of data points in the lower portion of Fig. 6 display the composition dependence of the properly normalized Raman intensities of the 69- and 80-cm^{-1} K β-alumina cation vibrations. Both modes exhibit highly nonlinear dependence upon K^+ concentration which is fit below to the x dependence for site occupancy appearing in Table I. It is apparent from Fig. 6 that the rapid disappearance of the 69-cm^{-1} mode (relative to the 80-cm^{-1} mode) with decreasing K^+ content (as seen in the Raman spectra of Fig. 2 and correspondingly in Fig. 4 for the Na-Rb system) is due to the fact that near the K-rich end, (a) the 69-cm^{-1} intensity is decreasing rapidly and (b) the 80-cm^{-1} intensity is actually *increasing*. Both of these trends are verified by the analogous composition dependence, shown in Fig. 7, of the integrated conductivities of the corresponding far-ir K^+ modes at 69 and 86 cm^{-1}. The qualitative correspondence noted earlier between the composition dependence of the Raman and far-ir spectral features (Figs. 2 and 3) is thus extended to the intensities of each of the component lines of the spectrum. This correspondence tends to further confirm our assumption that the composition dependence of the Raman or far-ir intensity of a given mode is due primarily to variations in the number of the corresponding type of site, rather than variations of the matrix elements involved in either type of measurement.

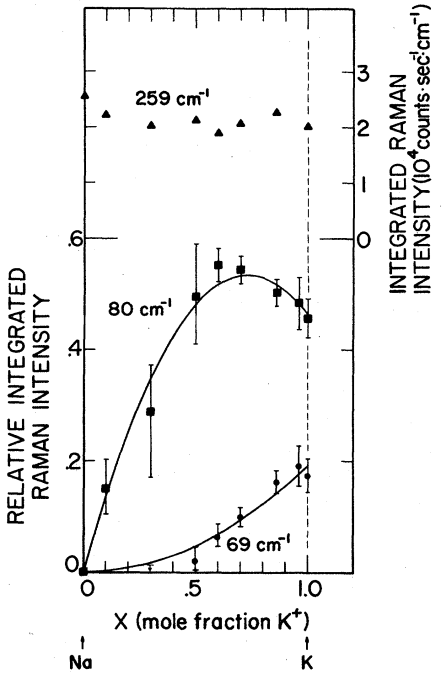

FIG. 6. Upper portion: composition dependence of the absolute integrated Raman intensity of the 259-cm^{-1} phonon used for the normalization of the Raman intensities of the cation modes in the $Na_{1-x}K_x$ mixed system. Lower portion: composition dependence of the (properly normalized) relative integrated Raman intensities of the 69- and 80-cm^{-1} K^+ modes. The data points were obtained by fitting the Raman spectra to a sum of Lorentzian line shapes. The error bars indicate the uncertainty in the fitting parameters at the 95% confidence level, as determined by the line-shape fitting program (Ref. 26).

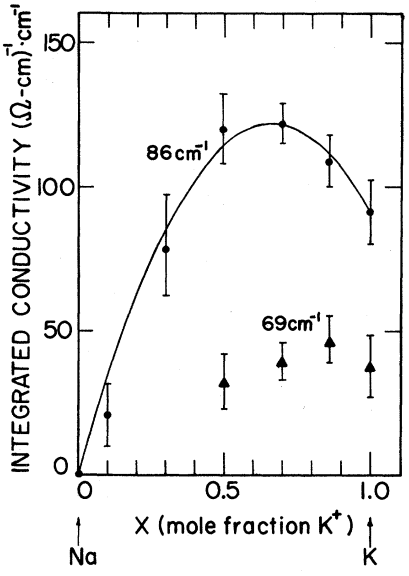

FIG. 7. Dependence upon K^+ concentration of the integrated far-ir conductivity associated with the 69- and 86-cm^{-1} far-ir modes of K β-alumina. The solid line is a least-squares fit for the 86-cm^{-1} mode to an $Ax^2 + Bx(1-x)$ dependence. As discussed in the text, a meaningful fit to the data for the 69-cm^{-1} mode could not be carried out due to excessive uncertainities in the associated integrated conductivities.

The solid lines in Fig. 6 are least-squares fits of the Raman intensities to functional dependencies from Table I. The 69-cm^{-1} K mode data are seen to be fit well by an x^2 dependence, and is thus consistent with an assignment to K-K pairs. The data points for the 80-cm^{-1} K mode, however, do not fit any single x dependence appearing in Table I. The only K-related site that would increase in number as K is replaced by Na is the Na-K pair, but the number of such pairs should vanish in pure K β-alumina ($x=1$). Therefore, the data for this mode have been fitted to a sum of contributions from both K-K and Na-K pairs; the fit is indicated by the solid line. Although the implicit assumption of degeneracy between the Na-K and K-K pair vibrational frequencies may make this assignment appear somewhat arbitrary, a recent calculation by Wang *et al.*[27] indicates that the vibrational frequencies for the two sites are separated by less than 1 cm^{-1}. Although the actual frequencies calculated (~52 cm^{-1}) are significantly lower than those observed (80 cm^{-1}), this discrepancy is not significant, as the absolute magnitudes of the calculated frequencies are expected to be less reliable than the result that the two frequencies are approximately equal.

The solid line in Fig. 7 represents a similar least-squares fit of the integrated intensity of the 86-cm^{-1} far-ir mode to a composition dependence appropriate to a sum of K-K and Na-K pairs. The data are fit well by this dependence, and the correspondence to the analogous dependence of the 80-cm^{-1} Raman mode in Fig. 6 is excellent. However, no such clear-cut correspondence may be made between the data for the 69-cm^{-1} far-ir mode and the observed x^2 dependence of the analogous Raman mode. Although there is good qualitative agreement between the x dependence of the two modes (e.g., Figs. 2 and 3), the lack of detailed correspondence between the compositional dependence of the integrated intensities is interpreted as resulting from the large error bars (e.g., Fig. 3) associated with the far-ir measurement as applied to a relatively weak spectral feature (for $x<0.86$) on the shoulder of the main 86-cm^{-1} absorption peak. The error associated with the analogous 69-cm^{-1} Raman mode is inherently smaller. Consequently, the dependence of the mode intensities upon K^+ concentration is deduced from the Raman spectra and verified by the far-ir measurements either quantitatively for the case of the strong 86-cm^{-1} mode, or qualitatively for the case of the weaker 69-cm^{-1} mode.

The results of the above analysis therefore indicate that for pure K β-alumina, the 69- and 80-cm^{-1} Raman modes are both due to vibrations of K-K pairs. This result corresponds well with the phonon calculation of Hsu.[22] Also, the strong correlation of the composition dependence (i.e., rapid decrease of the lower-frequency mode intensity with decreasing x) of this pair of modes with the analogous composition dependence of the pairs of K β-alumina far-ir modes (69 and 86 cm^{-1}, Fig. 3) and Rb β-alumina Raman modes (59 and 65 cm^{-1}, Fig. 4) indicates that all of these pairs of vibrational modes are of similar origin, i.e., doubly occupied sites. As a further inductive step, we note the correspondence of the Rb β-alumina far-ir spectrum of Allen *et al.*[9] [Fig. 4(a)] with both the Rb β-alumina Raman spectrum [Fig. 4(b)] and with the K β-alumina far-ir spectrum (Fig. 3). This similarity between the spectral features suggests that the 61- and 73-cm^{-1} modes in the Rb far-ir spectrum are probably of the same origin as the other pairs of modes discussed above. These results are summarized in Table II, where the spectral features associated with the various sites are identified by their observed vibrational frequencies.

An analysis similar to that in Fig. 6 has also been carried out for both the integrated Raman intensity (centered at 60 cm^{-1}) and the integrated far-ir conductivity (centered at 64 cm^{-1}) associated with the Na cation vibrations. As shown in Fig. 8, both sets of data exhibit a highly nonlinear dependence upon Na concentration that is fit well with a $(1-x)^2$ dependence. This suggests (Table I) that the most prominent feature of the Na β-alumina spectrum is also due to doubly occupied sites.

B. Singly occupied sites

The data analysis thus far has not dealt with modes due to singly occupied sites, although one expects such modes to represent about 60% of the total cation infrared oscillator strength (in the absence of cation-cation coupling). The infrared oscillator strength left unassigned at this point consists of a mode observed at 108 cm^{-1} in K β-alumina and a broad high-frequency tail (80–120 cm^{-1}) appearing most strongly at the Na-rich compositions. These two contributions were not

TABLE II. Association of spectral features observed in Na, K, and Rb β-alumina with specific cation sites. Spectral features are indicated by their observed vibrational frequencies (cm^{-1}).

Type of site		Na	K	Rb
Singly occupied	Raman	...	...	~90
	Infrared	80–120	108	87
Doubly occupied	Raman	~60	69, 80	59, 65
	Infrared	~64	69, 86	61, 73

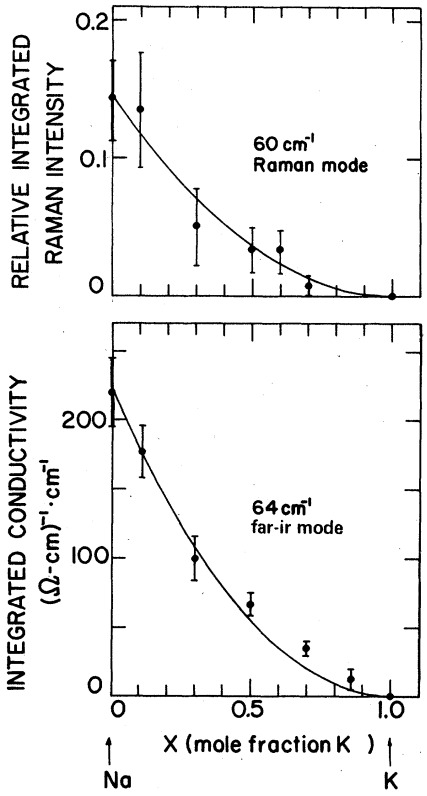

FIG. 8. Dependence upon K^+ concentration of (a) the integrated relative Raman intensity of the 60-cm^{-1} mode of Na β-alumina, and (b) the integrated far-ir conductivity of the 64-cm^{-1} mode of Na β-alumina. The solid lines in both cases are least-squares fits to a $(1-x)^2$ dependence.

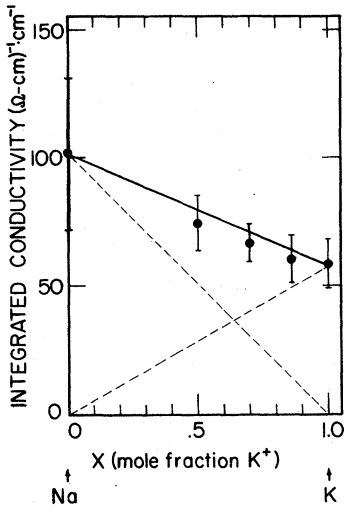

FIG. 9. Composition dependence of the sum of the integrated conductivities for the 108-cm^{-1} K^+ mode and the broad high-energy (80–120 cm^{-1}) tail of the Na^+ mode. The two contributions were difficult to separate uniquely by computer decomposition. The solid line shows the linear behavior expected from the sum of contribution from both Na and K BR sites (shown individually as the dashed lines). The solid line was constrained to agree with the experimental endpoints ($x=0$ and $x=1$).

separable with any degree of certainty over a sufficiently wide composition range to identify either component as due purely to Na or K unpaired cations. However, the total intensity of these two contributions, plotted in Fig. 9, can be fit well by a function $Ax+B(1-x)$, and is thus consistent with an assignment to contributions from a superposition of Na and K BR sites. This assignment is also consistent with the calculation by WGC of Na and K BR frequencies (90 and 98 cm^{-1}, respectively), both in overall magnitude and in the relative frequencies of the single-ion and pair modes.

The observed oscillator strength (integrated conductivity in the harmonic-oscillator approximation) of the high-frequency component does not amount to the expected 60% of the total; the fraction is closer to 40%. However, we have made detailed estimates of the effects of cation-cation coupling on the cation vibrational modes (taking the cation–spinel-block spring constant as a variable input parameter), and find that pair and single-ion modes at the assigned frequencies would mix to some extent, and that a significant amount of oscillator strength would tend to be transferred from higher-frequency single-ion modes into lower-frequency pair modes.[25] Employing a model with realistic (29%) cation excess, the results for several different arrangements of interstitial cation pairs were essentially the same: the single-ion sites, occupied by 56% of all the cations, accounted for only 45% of the total oscillator strength. Although the precise amount of transferred oscillator strength resulting from these calculations is certainly model dependent, it is clear that the magnitude of the observed oscillator-strength transfer can be accounted for by this mechanism. The assignment of the 108-cm^{-1} K infrared mode and the broad (80–120-cm^{-1}) Na infrared mode to BR sites is thus consistent with the observed compositional dependence, the expected relative oscillator strengths, and the calculated frequencies of WGC.

A Raman-active mode due to cations at BR sites is expected to be in the same frequency region as each of the far-ir modes discussed above. For example, the close correspondence between the K β-alumina Raman and far-ir spectra (Figs. 2 and 3) might suggest that the 98-cm^{-1} Raman mode is the Raman analog to the 108-cm^{-1} infrared mode, and is thus also attributable to BR sites. However, there are several arguments against this:

(i) the Raman mode appears in all β-aluminas at nearly the same frequency[5] with the exception of Rb, as mentioned previously; (ii) it corresponds well to the purely Raman-active mode calculated by Barker *et al.*[7] (108 cm^{-1}) and similarly assigned by Hao *et al.*,[5] as due to an in-plane oxygen vibration weakly coupled to the metal ions; (iii) it exhibits a very different dependence of vibrational frequency upon composition than does the 108-cm^{-1} infrared mode, as shown in Fig. 5. In contrast, the other Raman-infrared pairs show very strong correlations with composition.

It is therefore probable that the Raman analog of the 108-cm^{-1} infrared mode in K β-alumina is weak, and is obscured by the stronger 98-cm^{-1} phonon. To pursue this point further, a sensitive measurement of the Raman spectrum of Rb β-alumina was performed in the frequency region of the infrared BR mode (87 cm^{-1}). As discussed in Sec. III, a distinct shoulder was observed near 90 cm^{-1} [Fig. 4(b)]. The good correspondence of the frequency of this mode with the infrared frequency and with the predictions of WGC (78 cm^{-1}) makes it a good candidate for the Raman peak due to BR sites. Considering the significant decrease in ionic polarizability in the series Rb → K → Na, which corresponds with the observed decrease[5] in total Raman intensity, it would be expected that the corresponding Raman modes in K and Na β-alumina would be commensurately weaker. This trend would explain their absence from the observed Raman spectra in Na and K β-alumina. All of the assignments made in this section are summarized in Table II.

V. CONCLUSION

The assignments of spectral features to specific cation sites made in Sec. IV were based upon (i) the correspondence between the observed compositional dependence and that expected assuming an interstitialcy model with random occupation of excess cations on lattice sites; (ii) the close similarity between the observed compositional dependence of the Raman spectra in the Na-Rb system, the Raman spectra in the Na-K system, and the far-ir spectra in the Na-K system; (iii) the detailed comparison of corresponding spectral features in Na, K, and Rb β-alumina for both infrared and Raman measurements; (iv) the qualitative consistency of these assignments with the results of recent model calculations. The correspondence between the results in the three different isomorphs and two mixed systems and between the two experimental techniques gives internal consistency to these assignments. The results provide strong evidence for the existence of the correlated ion pairs treated by WGC. In fact, the most prominent features of the vibrational spectra have been interpreted in terms of correlated ion-pair vibrations.

The present results are thus inconsistent with the view[5] that the Raman spectra result primarily from the motion of unpaired BR ions within a superlattice structure. However, the role of local ordering in determining the details of the vibrational spectra of the β-aluminas is still not completely understood. In this regard, it is noteworthy that the calculated phonon spectrum[22] of nonstoichiometric K β-alumina in a superlattice structure contains new modes, relative to those calculated for stoichiometric β-alumina, that compare well to the sharp pair modes assigned in the present work. It is unclear, however, whether the sharp structure is due to the introduction (relative to the stoichiometric structure) of pairs or to the local ordering of the pairs. Comparison to the broad, featureless pair spectrum of the more disordered Na isomorph would tend to indicate the latter. An intriguing one-to-one correspondence between the presence of structure in the vibrational spectra and the widths of the diffuse x-ray-scattering peaks seems to support this view. Boilot *et al.*[17] have deduced from the diffuse x-ray-scattering measurements the temperature dependence of the ion-ion correlation lengths in Na, K, and Ag β-alumina, and find that the correlation lengths for Na and for Ag (300 K) are at least a factor of 2 smaller than those of K and Ag (4 and 77 K). The correlation length for Rb has already been measured[16] to be significantly larger than that of K, so that Rb also falls into the latter group. The vibrational spectra exhibit a one-to-one correspondence with this behavior; the Raman spectra in Na and Ag (300 K) are broad and featureless, while those of K, Rb, and Ag (4 and 77 K) are sharp and structured. The obvious implication is that the sharp structure in the pair-mode spectra is due to stronger ion-ion correlations, i.e., local ordering. However, this view should be taken with some caution. First, results inferred from measurements in Ag β-alumina should be weighed carefully in the present context, since the excess cations in the Ag isomorph occupy different sites than in Na, K, or Rb, and the superlattice structure for this material is also different. Also, recent diffuse x-ray measurements by McWhan *et al.*[18] indicate that the broad diffuse peaks observed for Na and Ag (300 K) may be due not only to static disorder resulting from the occupation of excess and compensating ions in interstitial sites, but also to dynamic disorder related to the cation motion.

ACKNOWLEDGMENTS

Two of us (P. B. Klein and D. E. Schafer) are grateful to the NRL–National Research Council

Resident Research Associate program for financial support. We would also like to thank S. J. Allen, D. B. McWhan, and Sang-il Choi for supplying preliminary versions of their papers prior to publication, and P. C. Taylor for a critical reading of the manuscript.

---

*Present address: Honeywell Material Sciences Center, Bloomington, Minn., 55420.

[1]M. S. Whittingham and R. Huggins, J. Chem. Phys. 54, 414 (1971); J. Electrochem. Soc. 118, 1 (1971).
[2]J. C. Wang, M. Gaffari, and Sang-il Choi, J. Chem. Phys. 63, 772 (1975).
[3]C. Peters, M. Bettman, J. Moore, and M. Glock, Acta Crystallogr. B 27, 1826 (1971).
[4]L. L. Chase, C. H. Hao, and G. D. Mahan, Solid State Commun. 18, 401 (1976).
[5]C. H. Hao, L. L. Chase, and G. D. Mahan, Phys. Rev. B 13, 4306 (1976).
[6]S. J. Allen, Jr., and J. P. Remeika, Phys. Rev. Lett. 33, 1478 (1974).
[7]A. S. Barker, Jr., J. A. Ditzenberger, and J. P. Remeika, Phys. Rev. B 14, 386 (1976).
[8]U. Strom, P. C. Taylor, S. G. Bishop, T. L. Reinecke, and K. L. Ngai, Phys. Rev. B 13, 3329 (1976).
[9]S. J. Allen, Jr., L. C. Feldman, D. B. McWhan, J. P. Remeika, and R. E. Walstedt, in *Superionic Conductors*, edited by G. D. Mahan and W. L. Roth (Plenum, New York, 1976), p. 279; S. J. Allen, Jr., A. S. Cooper, F. DeRosa, J. P. Remeika, and S. K. Ulasi, Phys. Rev. B 17, 4031 (1978).
[10]W. L. Bragg, C. Gottfried, and J. West, Z. Kristallogr. 77, 255 (1931).
[11]C. A. Beevers and S. Brohult, Z. Kristallogr. 95, 472 (1936).
[12]C. A. Beevers and M. A. S. Ross, Z. Kristallogr. 97, 59 (1937).
[13]W. L. Roth, F. Reidinger, and S. LaPlaca, in *Superionic Conductors*, edited by G. D. Mahan and W. L. Roth (Plenum, New York, 1976), p. 223.
[14]A. S. Barker, Jr., J. A. Ditzenberger, and J. P. Remeika, Phys. Rev. B 14, 4254 (1976).
[15]Y. LeCars, R. Comès, L. Deschamps, and J. Thery, Acta Crystallogr. A 30, 305 (1974).
[16]D. B. McWhan, S. J. Allen, Jr., J. P. Remeika, and P. D. Dernier, Phys. Rev. Lett. 35, 953 (1975).
[17]J. P. Boilot, G. Collin, R. Comès, J. Thery, R. Collongues, and A. Guinier, in *Superionic Conductors*, edited by G. D. Mahan and W. L. Roth (Plenum, New York, 1976), p. 243; J. P. Boilot, J. Thery, R. Collongues, R. Comès, and A. Guinier, Acta Crystallogr. Sec. A 32, 250 (1976).
[18]D. B. McWhan, P. D. Dernier, C. Vettier, A. S. Cooper, and J. P. Remeika, Phys. Rev. B 17, 4043 (1978).
[19]R. E. Walstedt, R. Dupree, and J. P. Remeika, in *Superionic Conductors*, edited by G. D. Mahan and W. L. Roth (Plenum, New York, 1976), p. 369.
[20]P. J. Anthony and A. C. Anderson, Phys. Rev. B 14, 5198 (1976).
[21]D. B. McWhan, C. M. Varma, F. L. S. Hsu, and J. P. Remeika, Phys. Rev. B 15, 553 (1977).
[22]William Y. Hsu, Phys. Rev. B 14, 5161 (1976).
[23]Y. Y. Yao and J. T. Kummer, J. Inorg. Nucl. Chem. 29, 2453 (1967).
[24]J. T. Kummer, Prog. Solid State Chem. 7, 141 (1976).
[25]Cation vibrational eigenvectors were calculated for a $\sqrt{7}\,a_0 \times \sqrt{7}\,a_0$ superlattice (a_0 is the β-alumina in-plane lattice constant). Such a superlattice allowed the introduction of a realistic cation excess (29%) as well as the corresponding number of excess in-plane oxygens (one per superlattice unit cell). Both direct (i.e., Coulomb) and indirect (via polarization of spinel-block ions) contributions to the cation-cation vibrational coupling were estimated. In calculating the self-consistent polarization response, the spinel-block ions were taken as point dipoles having the polarizabilities used in Ref. 2.
[26]The experimental spectra were fit to a sum of Lorentzian line shapes using the general least squares with statistics fitting program developed by Walter B. Daniels, Technical Report No. 579, University of Maryland, Dept. of Physics and Astronomy.
[27]J. C. Wang, D. F. Pickett, Jr., and Sang-il Choi, Bull. Am. Phys. Soc. 22, 370 (1977).